

REPORT DOCUMENTATION PAGE

Form Approved
OMB NO. 0704-0188

Public Reporting burden for this collection of information is estimated to average 1 hour per response, including the time for reviewing instructions, searching existing data sources, gathering and maintaining the data needed, and completing and reviewing the collection of information. Send comment regarding this burden estimates or any other aspect of this collection of information, including suggestions for reducing this burden, to Washington Headquarters Services, Directorate for Information Operations and Reports, 1215 Jefferson Davis Highway, Suite 1204, Arlington, VA 22202-4302, and to the Office of Management and Budget, Paperwork Reduction Project (0704-0188), Washington, DC 20503.

1. AGENCY USE ONLY (Leave Blank)		2. REPORT DATE 18 May 2001	3. REPORT TYPE AND DATES COVERED Final Technical 01 Mar 1999 – 29 Feb 2000
4. TITLE AND SUBTITLE Network Analyzer for Carrier Lifetime Measurements in Mid-IR Semiconductor Lasers		5. FUNDING NUMBERS DAAD19-99-1-0064	
6. AUTHOR(S) Lester, Luke F.		8. PERFORMING ORGANIZATION REPORT NUMBER 3-13381 FT	
7. PERFORMING ORGANIZATION NAME(S) AND ADDRESS(ES) The University of New Mexico Center for High Technology Materials, 1313 Goddard SE Albuquerque, NM 87106		10. SPONSORING / MONITORING AGENCY REPORT NUMBER 39396.1-EL-RIP	
9. SPONSORING / MONITORING AGENCY NAME(S) AND ADDRESS(ES) U. S. Army Research Office P.O. Box 12211 Research Triangle Park, NC 27709-2211		11. SUPPLEMENTARY NOTES The views, opinions and/or findings contained in this report are those of the author(s) and should not be construed as an official Department of the Army position, policy or decision, unless so designated by other documentation.	
12 a. DISTRIBUTION / AVAILABILITY STATEMENT Approved for public release; distribution unlimited.		12 b. DISTRIBUTION CODE	
13. ABSTRACT (Maximum 200 words) The Hewlett-Packard 8722D microwave network analyzer and cables that were obtained under the Grant have been used to perform the first electrical measurements of the carrier lifetime, τ_d , and radiative recombination in quantum dot LEDs. Our analysis shows that the ground and excited quantum dot energy states exhibit significantly different radiative recombination rates. We have measured τ_d as a function of current density for quantum dot LED samples using the microwave equipment and used this data to calculate the functional relationship between the carrier lifetime, carrier density, and radiative efficiency. The results indicate that carrier filling on the different dot energy levels has a strong influence on the radiative behavior of the devices and that the radiative rate coefficient, B , for different QD levels can vary considerably.			
14. SUBJECT TERMS Radiative recombination, Quantum dots		15. NUMBER OF PAGES 3	
		16. PRICE CODE NSP	
17. SECURITY CLASSIFICATION OR REPORT UNCLASSIFIED	18. SECURITY CLASSIFICATION ON THIS PAGE UNCLASSIFIED	19. SECURITY CLASSIFICATION OF ABSTRACT UNCLASSIFIED	20. LIMITATION OF ABSTRACT UL

NSN 7540-01-280-5500

Standard Form 298 (Rev. 2-89)
Prescribed by ANSI Std. Z39-18
298-102

20010619 086

Network Analyzer for Carrier Lifetime Measurements in Mid-IR Semiconductor Lasers

Final Report
Research Agreement No. DAAD19-99-1-0064

Summary statement: The Hewlett-Packard 8722D network analyzer and cables that were obtained with this DURIP grant money have been used to perform the first electrical measurements of the carrier lifetime and radiative recombination in quantum dot LEDs. Our analysis shows that the ground and excited quantum dot energy states exhibit significantly different radiative recombination rates.

Spontaneous emission and even lasing from excited state transitions can be readily observed in quantum dot (QD) devices at low current densities. This is a consequence of the low QD density and small density of states that forces the ground state gain to saturate rapidly. Such properties open new avenues for investigation. In this report, the carrier lifetime and radiation recombination rates are determined from experimental microwave measurements performed on an HP 8722D network analyzer. Distinctly different properties characterize the ground and excited state emission.

The differential carrier lifetime τ_d as function of pump current density, J , for quantum dot LED samples [1] were measured (Fig. 1) by using the technique reported in [2,3]. The total carrier density, n , and carrier lifetime τ_s were obtained from the measured τ_d using $n(I) = \frac{1}{qS} \int_0^I \tau_d(I') dI'$ and $\tau_s(I) = qn(I)/J$ [4]. Analysis shows that the carrier lifetime is a strong function of the pump level. Once J increases beyond 20 A/cm², i.e. typical lasing levels, τ_s decreases from 0.8 to 0.4 ns.

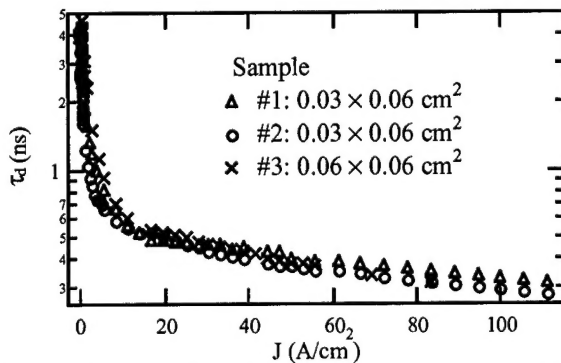


Fig. 1. Measured differential lifetime versus pump current for three QD LED samples.

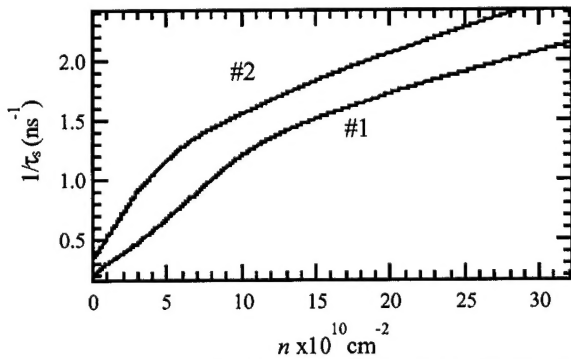


Fig. 2. Inverse carrier lifetime $1/\tau_s$ versus carrier density for two QD LED samples.

The recombination rate R is traditionally expressed in terms of the carrier density by $R = An + Bn^2$, where the coefficients A , and B characterize defect and radiative recombination respectively, and Auger recombination is insignificant. The recombination A and B coefficients can be obtained from $\tau_s^{-1} = R/n = A + Bn$. Thus a plot of $1/\tau_s$ versus n should yield a straight line

with an intercept of A and a slope of B , and this has been observed for some QW lasers [4]. However, the curve of $1/\tau_s$ versus n for the QD LED samples presents a clearly different behavior (Fig. 2) showing intersecting lines of different slopes in two pump regimes. Since these two pump regimes correspond to carrier filling mainly on the ground state and the 1st excited state, the different slopes in the plot of $1/\tau_s \sim J$ indicate that these two levels have different radiative recombination rates. This circumstance could be caused by lower wave-function overlap between electrons and holes involved in the 1st excited state transition. To account for these results, the total recombination rate R is generalized to reflect the carrier densities in the QD ground and excited states along with the QW ground state

$$R = \sum_{i=0}^2 (A_d \bullet n_{di} + B_{di} \bullet n_{di}^2) + (A_w \bullet n_w + B_w \bullet n_w^2).$$

Here A_d and B_{di} are A, B coefficients for QD states, and n_{di} is the 2D carrier density of the i th ($i=0$ is for the ground state, $i=1,2$ are for the 1st and 2nd excited states). The terms in the last brackets are the recombination rates associated with carrier filling in the lowest energy QW state. The total carrier density n is the sum of the component densities, $n = n_{d0} + n_{d1} + n_{d2} + n_w$. The carrier concentrations n_{d0} , n_{d1} , and n_{d2} are found using discrete energy levels, and Fermi-Dirac statistics within the QDs and between the QDs and the QW is assumed [5]. However, a global Fermi level is not assumed, only a local one. In other words, the dots have the same average carrier density. The values of n_{d0} , n_{d1} , n_{d2} and n_w for a given n are obtained from these assumptions, and then R is calculated to fit the experimental $J (=qR)$ versus n . The A, B coefficients as fitting parameters obtained in the calculation are $A_d = (2.9 \pm 0.7) \times 10^8 \text{ s}^{-1}$, $B_{d0} = (3.2 \pm 0.3) \times 10^{-2} \text{ cm}^2 \text{ s}^{-1}$, $B_{d1} = (2.4 \pm 0.3) \times 10^{-2} \text{ cm}^2 \text{ s}^{-1}$ and $B_{d2} = (3.0 \pm 0.5) \times 10^{-2} \text{ cm}^2 \text{ s}^{-1}$ for QDs. In Fig. 3 the fitted $n \sim J$ curve (solid line) for sample #2 shows very good agreement with the experimental data (dashed line). The corresponding carrier densities in each of the QD energy levels are also plotted in Fig. 3. The curves show several regimes of carrier filling on different energy states for an increase in current density. For most pump levels in this measurement n_w in the QW state is a small number compared to the carrier density in the dots.

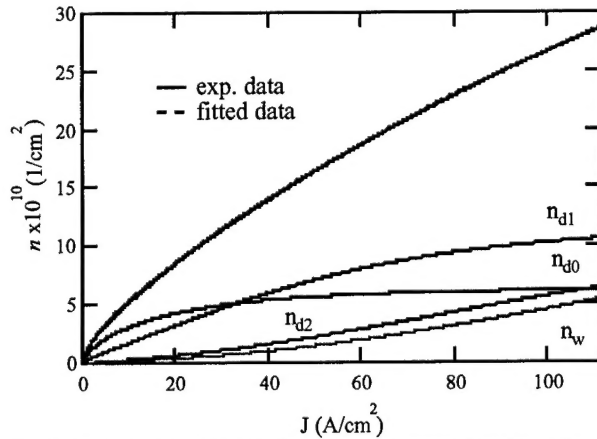


Fig. 3. The total carrier density n versus current density, J for experimental and theoretical data. Also shown are the carrier densities in the QD and QW states.

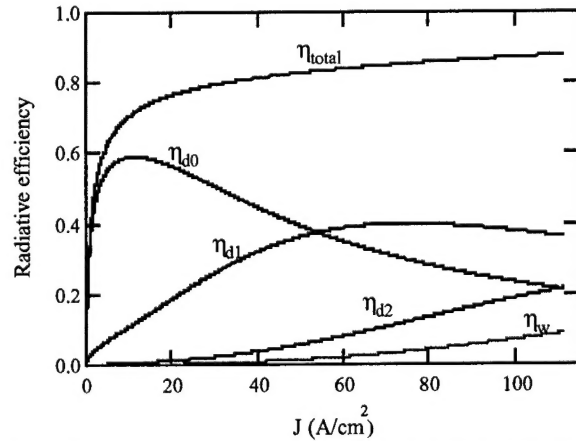


Fig. 4. Radiative efficiencies η versus pump current density J for emission from each state.

Figure 4 shows the radiative efficiency: $\eta_{d0} = B_{d0} n_{d0}^2 / R$ for the QD ground state, $\eta_{d1} = B_{d1} n_{d1}^2 / R$ for the QD 1st excited state, $\eta_{d2} = B_{d2} n_{d2}^2 / R$ for QD 2nd state, and $\eta_w = B_w n_w^2 / R$ for QW state. $\eta_{total} = \eta_{d0} + \eta_{d1} + \eta_{d2} + \eta_w$. Here R is the recombination rate defined above. The interesting result is that the radiative efficiency, η , for a particular QD state is strongly influenced by carrier filling in the

upper energy states. Therefore, the η will rise initially with increasing pump, reach a maximum, and then decrease with further increase in the pump as carrier filling saturates and occupation of higher energy states becomes significant.

In conclusion we have measured τ_d as a function of current density for QD LED samples using the microwave equipment purchased with the grant money and used this data to calculate the functional relationship between the carrier lifetime, carrier density, and radiative efficiency. The results indicate that carrier filling on the different dot energy levels has a strong influence on the radiative behavior of the devices and that the radiative rate coefficient, B , for different QD levels can vary considerably.

- [1] G. T. Liu, A. Stinz, H. Li, K. J. Malloy, and L. F. Lester, *Electron Lett.*, vol. 35, pp.1163-1165, 1999.
- [2] G. E. Shtengel, D. A. Ackerman, P. A. Morton, E. J. Flynn, and M. S. Hybertsen, *Appl. Phys. Lett.*, vol. 67, pp.1505-1508, 1995.
- [3] G. E. Giudice, D. V. Kuksenkov, H. Temkin, and K. L. Lear, *Appl. Phys. Lett.*, vol. 74, pp. 899-901, 1999.
- [4] R. Olshansky, C.B. Su, J. Manning, and W. Powazinik, *IEEE J. Quant. Electron.*, vol. QE-20, pp. 838-854, 1984.
- [5] H. Jiang and J. Singh, *J. Appl. Phys.*, vol. 85, pp.7438-7442, 1999.